

DMD #8078

Title:

S-2-pentyl-4-pentynoic hydroxamic acid and its metabolite S-2-pentyl-4-pentynoic acid in the NMRI-*exencephaly*-mice model: pharmacokinetic profiles, teratogenic effects, and histone deacetylase inhibition abilities of further VPA hydroxamates and amides.

Authors:

Daniel Eikel, Katrin Hoffmann, Karolin Zoll, Alfonso Lampen and Heinz Nau *

DE, KZ, HN

University of Veterinary Medicine Hannover - Foundation -, Center for Systemic Neuroscience Hannover, Centre for Food Science, Department of Food Toxicology and Chemical Analysis - Food Toxicology -, Bischofsholer Damm 15, D-30173 Hannover, Germany

KH

University of Veterinary Medicine Hannover - Foundation -, Center for Systemic Neuroscience Hannover, Institute of Pharmacology, Toxicology and Pharmacy, Bünteweg 17, D-30173 Hannover, Germany

AL

Federal Institute for Risk Assessment (BfR), Department of Food Safety, Thielallee 88 – 92, D-14195 Berlin, Germany

DMD #8078

Running Title:

Pro-teratogenic VPA derivatives

Corresponding Author:

Prof. Dr. Dr. h.c. Heinz Nau

University of Veterinary Medicine Hannover - Foundation -

Center for Systemic Neuroscience Hannover, Center for Food Science,

Department of Food Toxicology and Chemical Analysis - Food Toxicology -

Bischofsholer Damm 15

30173 Hannover – Germany

Email: Heinz.Nau@tiho-hannover.de

Tel.: 0049-511-856-7600

Fax.: 0049-511-856-7680

Number of text pages:	27
Number of tables:	7
Number of figures:	4
Number of references:	23
Number of words in abstract:	247
Number of words in Introduction:	484
Number of words in Discussion:	939

DMD #8078

Abstract:

Structure-activity relationship (SAR) studies of valproic acid (VPA) derivatives have revealed a quantitative correlation between histone deacetylase (HDAC) inhibition and induction of neural tube defects (NTDs) in the NMRI-*exencephaly*-mouse model, but this correlation was so far limited to congeners with a carboxylic acid function. Whereas the classical HDAC inhibitor Trichostatin A is active only as a hydroxamate but not as a carboxylic acid, we found that neither VPA amides nor hydroxamates inhibit HDACs, but can cause NTDs; e.g. 2-Pentyl-4-pentynoic hydroxamic acid with its *S*-enantiomer being the potent teratogen. We therefore investigated the hypothesis that hydroxamic acid derivatives of VPA might be metabolized in vivo and possibly pro-teratogenic as had been shown for valpromide but not valproic hydroxamic acid. We developed two stereoselective quantification methods based on chiral derivatization of VPA hydroxamates with (1*R*,2*S*,5*R*)-(-)-menthylchloroformate and carboxylic acid derivatives with (*S*)-(-)-1-naphthylethylamin followed by GC-NPD analysis of biological samples. We then determined the pharmacokinetic profiles of *S*-2-pentyl-4-pentynoic hydroxamic acid and of *S*-2-pentyl-4-pentynoic acid in mice. *S*-2-pentyl-4-pentynoic hydroxamic acid was found to be extensively metabolized to the corresponding carboxylic acid without affecting the stereochemistry at position C2. Furthermore the metabolite *S*-2-pentyl-4-pentynoic acid was found to be very stable in vivo with an extended half life of 4.2 h compared to that of VPA with 1.4 h. Comparison of the individual HDAC inhibition abilities of further VPA amides and hydroxamates, as measured by cellular and enzymatic assays, led us to the conclusion that both classes of VPA derivatives can be pro-teratogenic.

DMD #8078

Introduction:

Valproic acid (VPA) has been shown to be an inhibitor of histone deacetylases (HDACs), enzymes with a fundamental impact on chromatin remodeling and gene expression of cells (Phiel et al. 2001, Göttlicher et al. 2001). HDACs have chiefly been of interest as possible molecular targets for the treatment of cancer diseases (Yoshida et al., 2001). However in light of reports that further structural derivatives of VPA were HDAC inhibitors only if they were also teratogenic (Gurvich et al., 2004; Eyal et al., 2005) it has been suggested that VPA might also induce embryonic malformations by its inhibition of HDAC (Gurvich et al., 2005; Eikel et al., 2006), and this possibility has led to new interest in HDACs as molecular targets in toxicology. Recently we used the NMRI-*exencephaly*-mouse-model (Nau et al. 1981) to demonstrate a quantitative correlation between embryonic malformation and the HDAC inhibition potential of a set of 20 structurally diverse VPA derivatives (Eikel et al. 2006). We showed that the structural prerequisites allowing VPA derivatives to inhibit HDACs are unique and have previously not been shown for other classical HDAC inhibitors such as trichostatin A (TSA) or suberoylanilino-hydroxamic acid (SAHA).

Both TSA and SAHA have been shown to use their hydroxamic acid function to inhibit HDACs by complexing the catalytically active zinc atom of HDACs (Finnin et al., 1999; Somoza et al., 2004; Vannini et al., 2004). It was also shown that TSA and some structural derivatives are active only as hydroxamic acids but not as carboxylic acids or amides (Yoshida et al., 1990; Jung et al., 1999) which raises the question of whether valproic acid derivatives with hydroxamic acid function might be even more potent HDAC inhibitors than the corresponding carboxylic acids.

On the other hand it was shown that valproic hydroxamic acid (VPA-HA) was not teratogenic in the NMRI-*exencephaly*-mouse model, whereas 2-pentyl-4-pentynoic

DMD #8078

hydroxamic acid induced this specific embryonic malformation (Volland, 2002; Gravemann, 2002). Furthermore valpromide (VPD), the slightly teratogenic amide derivative of VPA, had been shown to be metabolized to VPA in vivo (Radatz et al., 1998) whereas valproic hydroxamic acid was shown not to be hydrolyzed (Levi et al., 1997). This raised the question of whether a hydrolysis might be the reason for the teratogenic effects of VPA hydroxamates.

Therefore we firstly investigated the HDAC inhibition potential of selected VPA derivatives that have amide and hydroxamic acid functions, and compared these data with the teratogenic potential of these derivatives measured in the *NMRI-exencephaly*-mouse-model. As no correlation between HDAC inhibition and teratogenic potency was found in our initial trials we also investigated the pharmacokinetic profile of a pair of most interesting hydroxamic and carboxylic acid derivatives of VPA. Our findings suggest that VPA derivatives with hydroxamic acid function can be extensively metabolized to the corresponding carboxylic acid, thus indicating that both valproic acid amides and valproic hydroxamic acids might be pro-teratogens depending on the teratogenicity of the corresponding carboxylic acid metabolite.

Materials and Methods:

Chemicals and Reagents.

All chemicals and reagents used were of analytical grade if not stated otherwise. Valproic acid, Cremophor EL, (1*R*,2*S*,5*R*)-(-)-menthylchloroformate and (S)-(-)-1-naphthylethylamine were obtained from Sigma Aldrich GmbH, Germany. Valpromide was a kind gift from Katwijck Chemie, The Netherlands. The VPA structural derivatives used in this study were synthesized according to methods published elsewhere (Radatz et al., 1998; Levi et al., 1997; Gravemann 2002; Nau 1985) or as described below (Figure 1).

Synthesis of valproic hydroxamic acid (I) and (±)-, *R*- and *S*-2-pentyl-4-pentynoic hydroxamic acid (VI, VIII, X)

The hydroxamic acid derivative of VPA and some of its selected congeners were synthesized by activation of the carboxylic acid group to the carboxylic acid chloride and conversion to the corresponding hydroxamate using hydroxylamine as reagent (Levi et al., 1997; Gravemann 2002). 50 mmol of reactant were dissolved in 15 mL thionyl chloride and boiled for 5 h at 90 °C under reflux. After cooling, the excessive thionyl chloride was removed under slight vacuum, and the carboxylic acid chloride distilled under high vacuum (10 mbar, at between 90 and 110 °C). The purified carboxylic acid chloride was then dissolved in 80 mL dry tetrahydrofuran and added slowly to a 5 °C solution of hydroxyl amine hydrochloride (1 mol), triethylamine (140 mL) and water (300 mL). The solution was stirred for another 1.5 h, and the hydroxamic acid product was extracted three times with 150 mL ethylene chloride. The combined organic solvents were washed with 80 mL hydrochloric acid solution (1 M) and dried for 12 h by stirring over sodium sulfate. The solution was filtered, the

DMD #8078

solvent evaporated to dryness, and the remaining red oil was flash-chromatographed on silica (Si 60 Machery-Nagel GmbH-Germany) with a 20:80 (v/v) mixture of ethyl acetate and ligroin. Product control of the eluate was performed using DC chromatography (Alugram Sil G/UV₂₅₄ Macherey-Nagel GmbH, Germany), and solvent fractions containing the product were combined and evaporated to dryness. After re-crystallisation in a 1:99 (v/v) mixture of ethyl acetate and ligroin the hydroxamic acid product was obtained as fine colorless crystals.

Results of the analytical procedures for the characterization of the substances under investigation here:

Valproic hydroxamic acid (VPA-HA, III):

Thin layer chromatography with a 50:50 (v/v) mixture of ethyl acetate and ligroin as solvent: $R_f(\text{VPA-HA})=0.5$, $R_f(\text{VPA})=1.0$; melting point: 123 °C; elemental microanalysis: $\text{C}_8\text{H}_{17}\text{NO}_2$ ($M_w=159.23$ g/mol) calculated: 60.35% C, 10.76% H, 8.80% N; measured: 60.35% C, 10.62% H, 8.76% N;

Nuclear magnetic resonance ^{13}C -NMR (100 MHz, δ): 14.0 (C5 and C5'); 20.7 (C4 and C4'); 34.7 (C3 and C3'); 44,0 (C2); 174.2 (C1)

Nuclear magnetic resonance ^1H -NMR (400 MHz, δ): 0.89 (t, 6H, $J=7.2$ Hz); 1.20-2.02 (m, 9H); 8.20 (bs, 1H); Infrared spectroscopy IR (ATR, ν (cm^{-1})): 3175 (br); 3027 (br); 2957 (s); 2929 (s); 2874 (s); 1626 (s); 1538 (s); 1464 (s); 1041 (s); 949 (s)

Mass spectrometry MS (70 eV, m/z (%)): 159 (42) M^+ ; 130 (16) $\text{M}^+-\text{C}_2\text{H}_5$; 127 (100) M^+-NHOH ; 117 (31) $\text{M}^+-\text{C}_3\text{H}_6$; 116 (17) $\text{M}^+-\text{C}_3\text{H}_7$; 99 (72) M^+-CONHOH ; 88 (58); 83 (46); 72 (57)

Chemical purity as measured by standard GC-MS analysis of the TMS ether: > 99%

(±)-2-pentyl-4-pentynoic hydroxamic acid (VI):

DMD #8078

Thin layer chromatography with a 20:80 (v/v) mixture of ethyl acetate and ligroin as solvent: $R_f(2\text{-propyl-4-pentynoic hydroxamic acid})=0.3$, $R_f(2\text{-propyl-4-pentynoic acid})=0.7$

melting point: 66 °C; elemental microanalysis: $C_{10}H_{17}NO_2$ ($M_w=183.25$ g/mol)
calculated: 65.54% C, 9.35% H, 7.64% N; measured: 65.48% C, 9.22% H, 7.60% N

Nuclear magnetic resonance ^{13}C -NMR (100 MHz, δ): 14.0 (C7); 21.6 (C6); 22.4 (C1'); 31.5 (C4 or C3); 31.6 (C4 or C3); 43.5 (C2); 70.7 (C2'); 81,4 (C3'); 172.6 (C1)

Nuclear magnetic resonance 1H -NMR (400 MHz, δ): 0.87 (t, 6H, $J=6.9$ Hz); 1.29 (m, 6H); 1.51-1.76 (m, 2H); 2.06 (t, 1H, $J=2.6$ Hz); 2.23-2.48 (m, 3H); 8.70 (s, 1H); 9.05 (bs, 1H)

Infrared spectroscopy IR (ATR, ν (cm^{-1})): 3279 (m); 3189 (br); 3035 (br); 2919 (s); 2858 (s); 1626 (vs); 1538 (m); 1459 (w); 1111 (m); 1067 (m); 1012 (m); 1000 (m); 953 (m);

Mass spectrometry MS (70 eV, m/z (%)): 183 (23) M^+ ; 167 (14); 151 (100) M^+ -NHOH; 144 (12) M^+ - C_3H_3 ; 123 (16) M^+ -CONHOH; 113 (32) M^+ - C_5H_{11} ; 112 (26) M^+ - C_5H_{11} ; 97 (39); 81 (99); 67 (58)

Chemical purity as measured by standard GC-MS analysis of the TMS ether: > 99%

(R)-2-pentyl-4-pentynoic hydroxamic acid (VIII):

The physico-chemical parameters of the R-enantiomer were identical to those of the racemate given above. Specific optical rotation α measured at 20 °C with $c = 10.16$ mg/mL in chloroform: +8.8 (589 nm); +9.2 (578 nm); +10.2 (546 nm); +15.7 (436 nm); +21.0 (365 nm); optical purity as measured by GC-NPD analysis after chiral derivatisation with (1*R*,2*S*,5*R*)-(-)-menthylchloroformate showed an enantiomeric excess of > 98% ee.

DMD #8078

(S)-2-Pentyl-4-pentynoic hydroxamic acid (X):

The physico-chemical parameters of the S-enantiomer were identical to those of the racemate given above. Specific optical rotation α measured at 20 °C with $c = 10.03$ mg/mL in chloroform: -8.6 (589 nm); -8.8 (578 nm); -9.8 (546 nm); -15.6 (436 nm); -21.3 (365 nm); optical purity as measured by GC-NPD analysis after chiral derivatisation with (1*R*,2*S*,5*R*)-(-)-menthylchloroformate demonstrated an enantiomeric excess of > 98% ee.

Stereoselective quantification of S-2-pentyl-4-pentynoic hydroxamic acid (X) in biological samples.

Samples of plasma (50 μ L) or tissue (50 mg) were diluted with 200 μ L buffer solution (500 mM sodium dihydrogen phosphate adjusted to pH 5.0) in a 2-mL Eppendorf reaction vial, to which 20 μ L of internal standard solution was added (valproic hydroxamic acid 0.5 μ g/ μ L in 100 mM disodium hydrogen phosphate adjusted to pH 7.4). Tissue samples were also homogenized in this solution at maximum power for 5 min with a T8 mini-ultraturrax from (IKA GmbH, Germany).

For extraction of analytes 1000 μ L ethyl acetate was added and the sample was shaken for 15 min at room temperature before centrifugation for 5 min at 5 °C and 20 000 g. After rising to the surface the organic phase was pipetted into another 2 mL Eppendorf reaction vial and the extraction procedure was repeated with another 1000 μ L ethyl acetate. The organic phases were combined, 100 μ L acetonitrile were added, and the sample was evaporated to dryness at 40 °C under a nitrogen stream.

For derivatization 300 μ L toluene, 10 μ L pyridine and 5 μ L (1*R*,2*S*,5*R*)-(-)-menthylchloroformate were shaken for 60 min at room temperature. After

DMD #8078

derivatisation, 100 μL water were added, and the sample was shaken again for 5 min and centrifuged for 5 min at 5 $^{\circ}\text{C}$ and 20 000 g. The organic solvent phase at the surface was pipetted into an 1.5 mL Eppendorf reaction vial and approximately 50 mg disodium sulfate were added to the sample for desiccation by shaking the suspension for 30 min and centrifugation for 5 min at 5 $^{\circ}\text{C}$ and 20 000 g. The organic solution (approximately 200 μL) was pipetted into a GC-vial and 1 μL was transferred to GC-NPD analysis.

Gaschromatographic separation was performed using an Agilent HP 1 column (30 m x 320 μm inner diameter x 0.25 μm film) and the following temperature program: start at 80 $^{\circ}\text{C}$, hold for 3 min, heat at 30 $^{\circ}\text{C}/\text{min}$ to 220 $^{\circ}\text{C}$, hold for 0 min, heat at 2 $^{\circ}\text{C}/\text{min}$ to 270 $^{\circ}\text{C}$, hold for 0 min, heat at 30 $^{\circ}\text{C}/\text{min}$ to 320 $^{\circ}\text{C}$, hold for 5 min. Separation was performed using helium 5.0 as the carrier gas at a flow rate of 2.2 mL/min, followed by nitrogen selective detection (50 pA, 20 min equilibration time) on an auto-sample Agilent GC 6890 gas chromatography station.

Stereoselective quantification of S-2-Pentyl-4-pentynoic acid (IX) in biological samples.

Samples were prepared as above with the following variations: 30 μL internal standard solution was added (0.5 $\mu\text{g}/\mu\text{L}$ 3-ethyl-pentanoic acid in 100 mM disodium hydrogen phosphate adjusted to pH 7.4), and the organic solvents were pipetted into a disposable glass vial in which, due to the volatile nature of the internal standard, the organic solvents were not evaporated to dryness but to a final volume of between 50 and 100 μL .

For derivatization, 400 μL methylene chloride, 200 μL 1-hydroxybenzotriazole solution (2 mg/mL in a 99:1 (v/v) mixture of methylene chloride and pyridine), 200 μL

DMD #8078

1-(3-dimethyldiaminopropyl)-3-ethylcarbodiimide hydrochloride solution (2 mg/mL in methylene chloride), and 200 μ L S-(-)-1-naphthyl-ethyl-amine (2 mg/mL in methylene chloride) were added to the glass vial, which was then gently shaken for 90 min at room temperature. After derivatization, the solution was evaporated to dryness under a nitrogen stream and resuspended in 100 μ L GC-solution (an 80:20 (v/v) mixture of n-hexane and ethyl acetate); finally 1 μ L of the resuspended solution was injected into the GC.

Gas chromatographic separation was performed using an Agilent HP 5 MS column (30 m x 320 μ m inner diameter x 0.25 μ m film) and the following temperature program: start at 120 °C, hold for 2 min; heat at 20 °C/min to 220 °C, hold for 1 min; heat at 10 °C/min to 230 °C, hold for 12 min; heat at 60 °C/min to 325 °C, hold for 6 min. The separation was carried out with helium 5.0 as the carrier gas at a flow rate of 2.0 mL/min, followed by nitrogen selective detection (50 pA sensitivity, 20 min equilibration) on an auto-sample Agilent GC 6890 gas chromatography station.

Validation of the quantification methods

The linear calibration curves for both quantification methods were computed with the software package Valoo[®] from Analytik-Software GmbH, Germany, based on the above described procedure and analysis of 20 mouse plasma samples spiked with concentrations ranging from 5 μ g/mL to 1000 μ g/mL each. All samples were measured in duplicate and linearity of the calibration curve as well as Limit of Quantification (LOQ) and Limit of Detection (LOD) was computed based on these samples. Further validation was done by intra-day and inter-day analysis of spiked mouse plasma and mouse tissue samples as summarized in Table 1. These samples were analyzed with six (tissues) or eight (plasma) replications in one day as intra-day analysis of variation or on six (tissues) or eight (plasma) days in three consecutive

DMD #8078

weeks as inter-day analysis of variation. Values shown were the mean of four different concentrations in the range of 30 $\mu\text{g/mL}$ to 800 $\mu\text{g/mL}$ ($\mu\text{g/g}$ for tissues respectively).

Measurement of the plasma protein binding of S-2-pentyl-4-pentynoic acid (IX) and S-2-pentyl-4-pentynoic hydroxamic acid (X).

For plasma protein binding studies the compound under investigation was incubated for 1 h at 37 °C at the indicated concentrations in pooled human or mice blank plasma (additional control samples were incubated in 100 mM phosphate buffer pH 7.4 alone). After incubation one aliquot of each sample was quantified by the above analytical methods, and 500 μL of each plasma or control sample were filtered by centrifugation (1 min, 10000 g, 37 °C) in a membrane filter unit (Vivaspin 500, PES membrane, 5 kDa MWCO or Vivaspin 2, Hydrosart® membrane, 5 kDa MWCO, both from Vivascience GmbH, Germany). The centrifugation was stopped after 1 min with a filtrate volume of approximately 80 μL in order not to disturb the binding balance. The plasma protein binding was calculated relative to the concentration of the spiked plasma samples with four independent samples at each concentration. The total amount of plasma protein binding was calculated as the average plasma protein binding over the complete concentration range measured.

DMD #8078

Measurement of pharmacokinetic drug profiles in mice.

For the analysis of the pharmacokinetic profile of both *S*-2-pentyl-4-pentynoic hydroxamic acid (**X**) and *S*-2-pentyl-4-pentynoic acid (**IX**) female NMRI mice weighing between 28 and 36 g were randomly assigned into groups of three per time of interest. Each animal was weighed and injected subcutaneously (s.c.) or intraperitoneally (i.p.) with the volume of test solution necessary to yield a dosage of 0.80 mmol/kg or 1.50 mmol/kg, respectively. Prior to injection the compound under investigation had been dissolved in water to a final concentration of 0.80 mmol/10 mL or 1.50 mmol/10 mL respectively, and neutralized. The animals were anesthetized with diethyl ether at the indicated times, and blood samples were taken. The animals were then sacrificed to obtain further tissues such as liver, spleen, kidney and brain. Analysis of the biological samples was performed as above and the time-dependent concentration curves were analyzed using the WinNonLin 4 software package from Pharsight Corporation, US, with a non-compartment analysis approach and the liner trapezoidal rule for estimation of the compound half-life.

Reproductive toxicity assay in the NMRI-exencephaly-mouse-model.

The reproductive toxicity was determined for selected VPA derivatives and solvent-only samples in the NMRI-exencephaly-mouse-model described in detail elsewhere (Nau et al., 1981). In short: female NMRI mice weighing between 28 and 36 g were mated three hours on day 0; on day 8.25 of gestation, compounds dissolved in water or 25% (v:v) ChremophorEL adjusted to pH 7.4 were injected intraperitoneally. On day 18 of gestation, the animals were sacrificed, the uteri removed, and the number of implants and resorptions counted. Each foetus was weighed and inspected for external malformations. The exencephaly rate was calculated relative to the number of living foetuses. Data were computed using the software package SigmaStat 3.0

DMD #8078

from Aspire Software International, USA, with the Kolmogorov-Smirnov test for normality, the ANOVA for ranks, followed by Dunn's test for significance. Exencephaly rates were compared by the z-test. For both test methods, significance was assumed at p values lower than 0.05.

All efforts were made to minimize both the suffering and the number of animals used in this study. All procedures conducted were in accordance with the German Animal Welfare Act and were approved by the responsible governmental agency under the licence numbers 00/269 and 02/612.

Measurement of the teratogenic potency.

The exencephaly rate was determined as described above as the model parameter for teratogenicity. These values were considered with previously published exencephaly rates for all other VPA derivatives used in this study (Radatz et al., 1998; Bojic et al., 1998; Volland 2002) to establish an arbitrary range of teratogenic potency which is shown in Table 2. The decision criteria range from 0 (no detectable teratogenic potency) to +++++ (very high teratogenic potency). The corresponding teratogenic potency rating of each VPA derivative used in this study is summarized in Table 3.

Histone hyperacetylation in cell culture.

Teratocarcinoma F9 mice cells (American Type Culture Collection, Rockville, MD - USA) were cultured in Ham's F-12/DMEM medium containing 2 mM L-Glutamine, 10% (v/v) fetal bovine serum, 0.145 mM 2-mercaptoethanol and 100 U/mL penicillin/streptomycin (medium and supplements from GIBCO/Invitrogen GmbH, Germany). For the experimental set-up 10^6 cells were treated in triplicate by incubation at 37 °C in a humid air atmosphere with 5% (v/v) CO₂. After 6 h, cells

DMD #8078

were scraped from the bottom of the well, washed twice with PBS, dissolved in 100 μ L lysis-buffer (62.5 mM Tris/HCl pH 6.8, 2% sodium dodecylsulfate (w/v), 1% glycerin (v/v), 2.5 μ M dithio-DL-threitol, 250 μ M phenylmethanesulfonyl fluoride, 0.05 μ g/mL bestatin, 2 μ g/mL aprotinin, 0.05 μ g/mL leupeptin) and boiled immediately for 5 minutes at 90 °C. Then, 10 μ L of this cell lysate was separated by 15% SDS-polyacrylamide gel electrophoresis and transferred to a nitrocellulose membrane by semi-dry electroblotting. The blotted membrane was washed with TBS-buffer (2.4 g/L Tris/HCl, 8 g NaCl, pH 7.6) and blocked with TBS-buffer containing 3% nonfat dry milk (TBS-M) for 1 h at room temperature. The nitrocellulose membrane was incubated with a 1:2000 dilution of anti-acetyl histone H4 antibody (Upstate/Biomol GmbH, Germany) in TBS-M at 4 °C for 12 h. The membrane was washed once with TBS buffer and again incubated with a 1:5000 dilution of an anti-rabbit antibody (ECL-detection kit, Amersham Bioscience, Germany) in TBS-M for 1.5 hours at room temperature. Blots were washed three times with TBS-Buffer, once with a mixture of 0.05 % (v/v) Tween 20 and TBS-buffer and again three more times with TBS-buffer before antibodies were detected with the ECL detection kit according to the manufacturer's instructions.

HDAC inhibition human enzyme assay.

HDAC activity was measured by using an HDAC fluorescence activity assay kit (Biomol GmbH, Germany). As the enzymatic test system is pH-dependent, the compounds to be measured were first dissolved in water and neutralized before preparation of further dilution series with HDAC assay buffer. The dose-activity samples were tested with at least three repeats according to the manufacturer's instructions. In short, HeLa nuclear extracts (1 μ L of between 6 and 9 mg/mL total protein) were incubated with 500 μ M acetylated Fluo-de-Lys substrate in 50 μ L of

DMD #8078

assay buffer in the presence or absence of the respective valproic acid analogue. The HDAC-inhibitor trichostatin A (TSA) at a concentration of 5 μM served as positive control. The deacetylation reaction was carried out at 37 $^{\circ}\text{C}$ for 3 h and stopped by addition of 50 μL Fluo-de-Lys developer solution containing 2 μM trichostatin A. After 15 min, fluorescence activity was measured with a Victor 1420 fluorescence reader (Perkin-Elmer LAS GmbH, Germany) at 355 nm excitation and 535 nm emission. The enzyme activity was calculated relative to the measured fluorescence activity of four negative controls (HDAC assay buffer only) on each 96-well plate. Determination of the $\text{IC}_{50}(\text{HDAC})$ value was computed, fitting at least six data points to a mathematical enzyme inhibition function with the pharmacodynamic module of the WinNonLin 4 software package (Pharsight Corporation, USA) to give IC_{50} values in $\mu\text{mol/L}$ with a standard error (SE) in $\mu\text{mol/L}$, which represents the goodness of fit between the computational model and the experimental data.

DMD #8078

Results:

The method employed here to synthesize hydroxamic acids from the chemically and optically pure carboxylic acid derivatives of VPA resulted in all cases in excellent yields of between 80% and 90%, and with chemical and optical purities > 99% (98% ee). We further developed two quantification methods for the stereoselective determination of VPA hydroxamates and carboxylic acids via chiral derivatization followed by GC-NPD analysis. These methods were used to investigate the pharmacokinetic profile of *S*-2-Pentyl-4-pentynoic hydroxamic acid and its potential metabolite, *S*-2-Pentyl-4-pentynoic acid.

Both analytes were obtained from biological samples by ethyl acetate liquid-liquid extraction at pH 5.0 (Hauck et al., 1992). The carboxylic acid was then derivatized in a classical approach using a chiral amine, (*S*)-(-)-1-naphthylethylamine. The hydroxamate was derivatized using (2*R*,3*S*,5*R*)-(-)-menthylchloroformate as the derivatization reagent, which resulted in a stable carbonate. Both analytes were separated from their corresponding enantiomer by GC and determined by NPD detection (Figure 2). Validation of both methods in a variety of biological matrices showed that kidney samples could not be tested for *S*-2-pentyl-4-pentynoic hydroxamic acid due to an unknown by-product of the derivatization process which crystallized inside the GC liner and blocked the injection port immediately after sample injection. Furthermore, there was a reproducible and significant signal enhancement of approximately 30% when liver samples were analyzed for *S*-2-pentyl-4-pentynoic acid, but these effects were not further investigated in this study. The overall evaluation of the two analytical procedures is summarized in Table 1 and shows the good reliability of both quantification methods.

Prior to the investigation of the pharmacokinetic profile of these two VPA derivatives we measured the plasma protein binding property of both *S*-2-pentyl-4-pentynoic

DMD #8078

hydroxamic acid and its hypothetical metabolite S-2-penty-4-pentynoic acid (Table 4). It could be shown that plasma protein binding of the carboxylic acid was between 20% and 25% higher than those of the hydroxamic acid, which supports the assumption that protein binding increases with increasing ionization at physiological pH. The average plasma protein binding of S-2-pentyl-4-pentynoic acid is 91% in human and 69% in spiked mouse plasma, values that are clearly higher than the plasma protein binding of VPA (80% and 12% respectively (Löscher 1999)). Both compounds also exert higher plasma protein binding in human plasma than mice plasma, which is in agreement to plasma protein binding data reported for VPA in both species (Löscher 1999).

Using the above analytical quantification methods we analyzed the pharmacokinetic profiles of both selected VPA derivatives (Table 5). Concentration time curves of S-2-pentyl-4-pentynoic hydroxamic acid in mice after i.p. dosage of 0.8 mmol/kg revealed that the compound is rapidly transported into the brain, where concentrations were even higher than plasma concentrations 1 h after injection (Figure 3a). Assuming that only the free drug could penetrate the blood brain barrier (BBB) and taking into account the 45% plasma protein binding of S-2-pentyl-4-pentynoic hydroxamic acid, these results indicate a slight accumulation of this VPA derivative in the brain without any significant hindrance to cross the BBB .

Further analysis of the pharmacokinetic values of S-2-pentyl-4-pentynoic acid after s.c. dosage of 1.5 mmol/kg revealed that this VPA derivative can also pass the BBB (Figure 3b). The brain concentrations were approximately 40% of plasma concentrations. Again keeping in mind the elevated plasma protein binding of 69%, it appears that there was no significant hindrance to BBB crossing.

Further pharmacokinetic parameter analysis of the plasma concentration time curves in a non-compartment model approach demonstrated that S-2-pentyl-4-pentynoic

DMD #8078

acid has a significantly enhanced half-life of 4.24 h, whereas that of the corresponding hydroxamate is only 0.33 h (Table 6). This analysis also showed a very high clearance of the hydroxamate and therefore a short mean residence time (MRT) of only 0.54 h, which can be explained by its rapid and extensive biotransformation to the corresponding carboxylic acid (Figure 4). After 30 min the metabolite plasma concentration was even greater than that of the parent hydroxamic acid; furthermore, due to its prolonged half life, the metabolite could still be detected after 6 h, whereas the parent drug was no longer detectable after 2 h. Analysis of the chromatographic data of plasma and tissue samples showed that the metabolic process did not affect the chiral centre at C2, nor did parent drug or metabolite convert their chiral center in vivo (data not shown).

R- and *S*-2-pentyl-4-pentynoic hydroxamic acid were both tested for their embryo toxic potential in the NMRI-*exencephaly*-mouse-model described above; the results indicated that only the *S*-enantiomer has teratogenic potency (Table 7). The poor water solubility of these VPA hydroxamates initially limited the dosage given to 0.80 mmol/kg. At this dosage, *R*-2-pentyl-4-pentynoic hydroxamic acid was neither embryo toxic by means of embryo lethality nor teratogenic with respect to the *exencephaly* endpoint. On the contrary average embryonic weight was significantly increased. But even at this low concentration the corresponding *S*-enantiomer led to a significant increase in embryo lethality of up to 19% and to an *exencephaly* rate of 2%, which is well above the spontaneous *exencephaly* rate of approximately 0.5% in this mice strain (Radatz et al., 1998; Bojic et al., 1998). With CremophorEL (25 %, v/v) as solubility enhancer it was possible to extend the dosage to 1.50 mmol/kg. The solvent enhancer did not increase the spontaneous *exencephaly* rate of the NMRI-mice strain (Table 7). CremophorEL 25 % (v/v) is also maternally non toxic but increases embryo lethality up to 13% compared to 5% embryo lethality when dosing

DMD #8078

saline solution as control. With this solubility enhancer, a dose of 1.50 mmol/kg S-2-pentyl-4-pentynoic hydroxamic acid induced a significantly higher rate of 5% exencephalies, while the corresponding R-enantiomer did not cause this form of malformation. The embryo lethality of the S-enantiomer was also higher than that of the R-enantiomer, but not significantly different from that of the control group. Since valproic acid and its teratogenic derivatives normally lead to quite steep increases on exencephaly rates depending on the dose (Nau 1985) it is likely that Cremophor EL reduced the teratogenic effects of S-2-pentyl-4-pentynoic hydroxamic acid. Although the dose was nearly doubled from 0.80 to 1.50 mmol/kg, the exencephaly rate increased only slightly from 2% to 5%. Such an effect might be due to influences of the solvent enhancer on both the biological availability and pharmacokinetics of the dissolved test compound.

We compared the above exencephaly rates for both enantiomers of 2-pentyl-4-pentynoic hydroxamic acid with previously published rates for all VPA derivatives used in this study and converted all rates into the arbitrary range of teratogenic potency. We also measured the HDAC inhibition ability of each compound both in an F9 cell culture assay and an HDAC human enzyme inhibition assay as described above, and compared the properties of these two compounds (Table 3). It was apparent that, regardless of the optical conformation, both amide and hydroxamic acid derivatives of VPA were not HDAC inhibitors at concentrations up to 2 000 μ M, and did not induce H₄ hyperacetylation in the F9 cell system. Nevertheless some members of both groups of VPA derivatives had been rated as slightly teratogenic (**II**, **V**, **VI** and **X**).

In light of the above-mentioned findings that VPA hydroxamates can be metabolized to the corresponding acids, we conclude that both amides (Radatz et al. 1998) and

DMD #8078

hydroxamates can be pro-teratogens if the in-vivo biotransformation leads to corresponding VPA carboxylic acids that are teratogenic.

DMD #8078

Discussion:

Currently, there is speculation about the possibility that both the teratogenic and anti-cancer effects of VPA are mediated by the inhibition of HDACs, an enzyme class crucially important for chromatin remodeling and expression of specific genes (Phiel et al., 2001; Göttlicher et al., 2001; Blaheta et al., 2005; Gurvich et al., 2005; Menegola et al., 2005). Support for the hypothesis that there is an interrelation between HDAC inhibition and teratogenic effects is provided by SAR studies on VPA derivatives demonstrating that teratogenic congeners are in fact at the same time HDAC inhibitors (Eikel et al., 2006; Eyal et al., 2005; Gurvich et al., 2004). Here we demonstrated that VPA hydroxamates and amides are no HDAC inhibitors, unlike trichostatin A (TSA) and suberoylanilidhydroxamic acid (SAHA), which are HDAC inhibitors only as hydroxamates but not as amides or carboxylic acids (Jung et al., 1999; Yoshida et al., 1990). We detected neither any hyperacetylation in F9 teratocarcinoma mice cells at concentrations up to 1 mM nor any functional inhibition of human HDAC enzymes at concentrations up to 2 mM. This fact suggests that VPA derivatives have a unique property for binding to HDAC enzymes not yet been described for other groups of known HDAC inhibitors.

But we also demonstrated that hydroxamic acid derivatives of VPA can indeed be teratogenic. The S-enantiomer of the chiral pair of VPA hydroxamates investigated here can induce teratogenic effects in the NMRI-*exencephaly*-mouse-model while the corresponding R-enantiomer does not. This is in good agreement with results of other studies of VPA carboxylic acid derivatives (Göttlicher et al., 2001; Eikel et al., 2006). Similarly Valpromide, the amide derivative of VPA, has teratogenic effects in vivo (Radatz et al., 1998) but is not able to inhibit HDAC. At first both these observations somewhat challenge the validity of the hypothesis that VPA exerts its teratogenic effects by inhibiting HDAC.

DMD #8078

But in light of previous reports of the *in vivo* metabolism and biotransformation of valpromide to valproic acid (Radatz et al., 1999), we hypothesized that VPA hydroxamates are also be metabolized to the corresponding acids and therefore be metabolically activated *in vivo*. So far it has been reported that valproic hydroxamic acid is not metabolized to its carboxylic acid *in vivo* (Levi et al., 1997).

To investigate our hypothesis we first developed two quantification methods that enabled us to detect both the *S*-2-pentyl-4-pentynoic hydroxamic acid as well as the theoretical metabolite *S*-2-pentyl-4-pentynoic acid. Additionally we were able to investigate the possible conversion of the chiral centre at position C2. The latter is theoretically possible due to the close proximity of the chiral center to the reactive hydroxamate function. Both quantification methods were successfully validated, so that we were able to monitor the parent compound and its hypothetical metabolite in a variety of murine tissues.

Investigation of the pharmacokinetic profile of *S*-2-pentyl-4-pentynoic hydroxamic acid itself revealed that the stereogenic center at C2 is stable *in vivo* with no chiral conversion detectable. This VPA derivative is rapidly and extensively distributed into the brain, so that brain concentrations are equal to plasma concentrations within the first 2 h after application. Under the light of the measured plasma protein binding of 45%, *S*-2-pentyl-4-pentynoic hydroxamic acid shows an excellent passage of the blood-brain-barrier (BBB). This observation is in agreement with previous findings that the anticonvulsant activities of VPA hydroxamates are equal or even superior to that of valproic acid (Levi et al., 1997; Volland 2002).

Our results regarding the metabolization of *S*-2-pentyl-4-pentynoic hydroxamic acid (X) to its corresponding acid are different than previously reported results obtained with valproic hydroxamic acid (III) in dogs (Levi et al., 1997). However, species, entity and dosage differences contribute to these different results. Again, the metabolism

DMD #8078

did not affect the stereo center at position C2, and resulted in plasma concentrations of the metabolite which were even greater than those of the parent drug after 30 min. This metabolite might also contribute to the previously described anticonvulsant effects of 2-pentyl-4-pentynoic hydroxamic acid (Volland 2002).

A study of the pharmacokinetic profile of this metabolite, S-2-pentyl-4-pentynoic acid, revealed that its half-life in mice is 4.2 h, which is a nearly 4 times longer than that of VPA (Löscher 1999). Nor was any conversion of the chiral center at position C2 detected in that study. Both these properties (long half-life, non-conversion) demonstrate the metabolic stability of this VPA derivative. Such stability might be caused by the triple bond in position C4-C5 (Hauck et al., 1992), which possibly withdraws the compound from the fatty acid metabolism pathways.

S-2-pentyl-4-pentynoic acid can also be shown to be a very potent HDAC inhibitor with an $IC_{50}(\text{HDAC})$ of 50 μM , indicating that its activity is ten times higher than that of valproic acid itself. Due to metabolism the accumulated amount of S-2-pentyl-4-pentynoic acid after i.p. dosage of 0.8 mmol/kg of the parent hydroxamic acid was approximately 15% to 20% of the plasma concentrations reached after direct s.c. dosage of 1.5 mmol/kg. With respect to the fact that the metabolite S-2-pentyl-4-pentynoic acid is a remarkably potent HDAC inhibitor, we conclude that the teratogenic effects of S-2-pentyl-4-pentynoic hydroxamic acid are induced by its metabolite.

Overall we conclude that VPA hydroxamates can be metabolized to their corresponding acids in vivo and are therefore potential pro-teratogens, depending on the teratogenic potential of their corresponding carboxylic acid metabolite. This metabolic process can be held responsible for the teratogenic effects of S-2-pentyl-4-pentynoic hydroxamic acid in the NMRI-*exencephaly*-mouse model, thus suggesting that VPA hydroxamates are not intrinsically teratogenic, but can be activated in vivo.

DMD #8078

This study is further evidence of HDAC inhibition as a molecular target for the induction of embryonic malformation and makes hydroxamate derivatives of VPA interesting model compounds for further mechanistic studies of teratogenicity.

DMD #8078

Acknowledgements

We thank Mrs. McAlister-Hermann (University of Veterinary Medicine Hanover) for valuable suggestions and critical reading of the manuscript.

References

- Blaheta R.A., Michaelis M., Driever P.H., Cinatl J. Jr, (2005) Evolving Anticancer Drug Valproic Acid: Insights into the Mechanism and Clinical Studies. *Med Res Rev* 25:383-397
- Bojic U., Ehlers K., Ellerbeck U., Bacon C.L., O'Driscoll E., O'Connell C., Berezin V., Kawa A., Lepekhin E., Bock E., Regan C.M., and Nau H. (1998) Studies on the teratogen pharmacophore of valproic acid analogues: evidence of interactions at a hydrophobic centre. *Eur J Pharmacol* 354:289-299
- Eikel D., Lampen A., Nau H. (2006) Teratogenic effects mediated by inhibition of histone deacetylases: Evidence from the structure activity relationship of valproic acid derivatives. *Chem Res Toxicol* (accepted for publication)
- Eyal S., Yagen B., Shimshoni J., Bialer M. (2005) Histone deacetylase inhibition and tumor cells cytotoxicity by CNS-active VPA constitutional isomers and derivatives. *Biochem Pharmacol* 69:1501-1508
- Finnin M.S., Donigian J.R., Cohen A., Richon V.M., Rifkind R.A., Marks P.A., Breslow R., Pavletich N.P. (1999) Structures of a histone deacetylase homologue bound to the TSA and SAHA inhibitors. *Nature* 401:188-193
- Gottlicher M., Minucci S., Zhu P., Kramer O.H., Schimpf A., Giavara S., Sleeman J.P., Lo Coco F., Nervi C., Pelicci P.G., and Heinzl T. (2001) Valproic acid

DMD #8078

defines a novel class of HDAC inhibitors inducing differentiation of transformed cells. *EMBO J* 20:6969-6978

Gravemann U. (2002) Synthesis of achiral, racemic and enantiomerically pure Valproic acid derivatives with anticonvulsant, neurotoxic and teratogenic potency. Doctoral-Thesis University Hannover

<http://edok01.tib.uni-hannover.de/edoks/e01dh03/359589863.pdf>

Gurvich N., Berman M.G., Wittner B.S., Gentleman R.C., Klein P.S., Green J.B. (2005) Association of valproate-induced teratogenesis with histone deacetylase inhibition in vivo. *FASEB J.* 19:1166-8

Gurvich N., Tsygankova O.M., Meinkoth J.L., and Klein P.S. (2004) Histone deacetylase is a target of valproic acid-mediated cellular differentiation. *Cancer Res* 64:1079-1086

Hauck R.S., Elmazar M.M.A., Plum C., Nau H. (1992) The enantioselective teratogenicity of 2-n-propyl-4-pentynoic acid (4-yn-VPA) is due to stereoselective intrinsic activity and not differences in pharmacokinetics. *Toxicol Lett* 60:145-153

Jung M, Brosch G, Kollé D, Scherf H, Gerhauser C, Loidl P. (1999) Amide analogues of trichostatin A as inhibitors of histone deacetylase and inducers of terminal cell differentiation. *J Med Chem* 42:4669 – 4679

DMD #8078

- Levi M., Yagen B., and Bialer M. (1997) Pharmacokinetics and antiepileptic activity of valproyl hydroxamic acid derivatives. *Pharm Res* 14:213-217
- Löscher W. (1999) Valproate: A reappraisal of its pharmacodynamic properties and mechanisms of action. *Prog Neurobiol* 58:31-59
- Menegola E., DiRenzo F., Broccia M.L., Prudenziati M., Minucci S., Massa V., Giovini E. (2005) Inhibition of histone deacetylase activity on specific embryonic tissues as a new mechanism for teratogenicity. *Birth Defects Res B Dev Reprod Toxicol* (electronic publication ahead of print)
- Nau H. (1985) Teratogenic valproic acid concentrations - Infusion by implanted minipumps vs conventional injection regimen in the mouse. *Toxicol Appl Pharmacol* 80:243-250
- Nau H., Zierer R., Spielmann H., Neubert D., and Gansau C. (1981) A new model for embryotoxicity testing: teratogenicity and pharmacokinetics of valproic acid following constant-rate administration in the mouse using human therapeutic drug and metabolite concentrations. *J Life Sci* 29:2803-2814
- Phiel C.J., Zhang F., Huang E.Y., Guenther M.G., Lazar M.A., and Klein P.S. (2001) Histone deacetylase is a direct target of valproic acid, a potent anticonvulsant, mood stabilizer, and teratogen. *J Biol Chem* 276:36734-36741

DMD #8078

Radatz M., Ehlers K., Yagen B., Bialer M., and Nau H. (1998) Valnoctamide, valpromide and valnoctic acid are much less teratogenic in mice than valproic acid. *Epilepsy Res* 30:41-48

Somoza J.R., Skene R.J., Katz B.A., Mol C., Ho J.D., Jennings A.J., Luong C., Arvai A., Buggy J.J., Chi E., Tang J., Sang B.C., Verner E., Wynands R., Leahy E.M., Dougan D.R., Snell G., Navre M., Knuth M.W., Swanson R.V., McRee D.E., Tari L.W. (2004) Structural snapshots of human HDAC8 provide insights into the class I histone deacetylases. *Structure* 12:1325-1334

Vannini A., Volpari C., Filocamo G., Casavola E.C., Brunetti M., Renzoni D., Chakravarty P., Paolini C., De Francesco R., Gallinari P., Steinkuhler C., Di Marco S. (2004) Crystal structure of a eukaryotic zinc-dependent histone deacetylase, human HDAC8, complexed with a hydroxamic acid inhibitor. *Proc Natl Acad Sci USA* 101:15064-15069

Volland J. (2002) Embryotoxicity, Anticonvulsant Action, Sedation and Adipocyte Differentiation: Structure-Activity-Studies with Valproic Acid Derivatives in Mice and C3H/10T1/2-Cells. PhD-Thesis University of Veterinary Medicine Hannover, Foundation
http://elib.tiho-hannover.de/dissertations/vollandj_2002.pdf

Yoshida M, Nomura S, Beppu T. (1990) Effects of trichostatins on differentiation of murine erythroleukemia cells. *Cancer Res.* 47:3688 - 3691.

DMD #8078

Yoshida M., Furumai R., Nishiyama M., Komatsu Y., Nishino N., Horinouchi S.

(2001) Histone deacetylase as a new target for cancer chemotherapy. *Cancer*

Chemother Pharmacol 48:S20-26

DMD #8078

Footnotes

We thank the Deutsche Forschungsgemeinschaft (Project DFG-NA 104/2-1), the European Research Training Network (Project RTN2-2001-00370), the European Commission (6th Framework Programme project: ReProTect), the Federal Ministry for Education and Research (BBF-Project 0313070D) and the Academy for Animal Health (ATF) for financial support.

Abbreviations:

HDAC(s), histone deacetylase(s); VPA, valproic acid; NTD(s), neural tube defect(s); H₄, core histone 4; ^{Ac}H₄, acetylated core histone 4; NMRI, Naval Medical Research Institute; IC₅₀(HDAC), inhibitor concentration with half maximum HDAC enzyme activity; NPD, nitrogen phosphor detector; GC, gas chromatography; SAR, structure-activity relationship; ATR IR, attenuated total reflection infrared spectroscopy

DMD #8078

Legends for Figures

- Figure 1** Chemical structures of the VPA derivatives investigated in this study (TSA and SAHA given for structural comparison).
- Figure 2** GC separation and NPD detection of the R and S enantiomers of both 2-pentyl-4-pentynoic hydroxamic acid (above, retention times 19.98 min and 20.04 min) and 2-pentyl-4-pentynoic acid (below, retention times 16.01 min and 16.48 min) after spiking of mouse plasma samples with 300 µg/mL, extraction process and derivatization with either (2*R*,3*S*,5*R*)-(-)-menthylchloroformate (MCF) or (S)-(-)-1-naphthylethylamine (NEA).
- Figure 3** Plasma and brain concentrations of S-2-pentyl-4-pentynoic hydroxamic acid after i.p. dosage of 0.80 mmol/kg (above) and of S-2-pentyl-4-pentynoic acid after s.c. dosage of 1.50 mmol/kg (below) in the NMRI mouse model.
- Figure 4** Plasma-concentration-time curves of S-2-pentyl-4-pentynoic hydroxamic acid and its metabolite S-2-pentyl-4-pentynoic acid after i.p. dosage of 0.8 mmol/kg of the hydroxamic acid in the NMRI mouse model.

Table 1 Validation parameters of the quantification methods for both S-2-pentyl-4-pentynoic hydroxamic acid and its metabolite S-2-pentyl-4-pentynoic acid.

Analyte	Matrix	Sample amount (μL or mg)	Linearity ($\mu\text{g}/\text{mL}$ or $\mu\text{g}/\text{g}$)	Coefficient of variation (%)	r^2	LOD ($\mu\text{g}/\text{mL}$ or $\mu\text{g}/\text{g}$)	LOQ ($\mu\text{g}/\text{mL}$ or $\mu\text{g}/\text{g}$)	Intraday (n = 6 or 8 samples)		Interday (n = 6 or 8 samples)	
								Mean- Recovery (%)	CV (%)	Mean- Recovery (%)	CV (%)
S-2-Pentyl-4-pentynoic hydroxamic acid X	Plasma	50	5 - 1000	5.5	0.997	5	14	103	2 - 4	103	5 - 10
	Brain	50						92	2 - 8	104	7 - 12
	Liver	50						93	8 - 11	104	10 - 14
	Kidney	--						--	--	--	
	Spleen	50						111	3 - 8	n.d. ¹	n.d. ¹
S-2-Pentyl-4-pentynoic acid IX	Plasma	50	5 - 1000	4.7	0.998	3	10	104	2 - 5	109	5 - 8
	Brain	50						90	2 - 3	92	3 - 4
	Liver	50						134	3 - 16	121	9 - 33
	Kidney	50						97	3 - 14	105	4 - 15
	Spleen	50						107	4 - 8	n.d. ¹	n.d. ¹

¹ not determined

DMD #8078

Table 2 Decision criteria for teratogenic potency rating of VPA derivatives investigated in the NMRI-*exencephaly*-mouse-model (Nau 1981).

Teratogenic potency	Dose range (mmol/kg)	Exencephaly rate (%)	Description
0	> 3.00	0	No teratogenic potency detectable
+	2.00 – 3.00	1 – 5	Low teratogenic potency
++	2.00 – 3.00	5 – 25	Lower teratogenic potency than VPA
+++	2.00 – 3.00	25 – 60	Equal teratogenic potency to VPA
++++	1.00 – 2.00	40 – 60	Higher teratogenic potency than VPA
+++++	0.25 – 1.00	40 – 60	Very high teratogenic potency

DMD #8078

Table 3 Teratogenic potency rating, H₄ hyperacetylation in treated F9 cells and HDAC enzyme inhibition ability of the VPA derivatives investigated in this study.

Compound	Teratogenic potency ¹ (0 - +++++)	IC ₅₀ (HDAC) ± SE ² (mM)	^{Ac} H ₄ -Hyperacetylation (0 - ++)
I	+++	400 ± 50	++
II	+ ³	> 2000	0
III	0	> 2000	+
IV	++++	35 ± 10	++
V	+	> 2000	0
VI	++	> 2000	0
VII	+++	870 ± 180	+
VIII	0	> 2000	0
IX	+++++	50 ± 12	++
X	++ ⁴	> 2000	0

¹ Data from the NMRI-*exencephaly*-mouse model inferred from Radatz et al., 1998; Bojic et al., 1998 and Volland 2002.

² SE representing the goodness of fit of the mathematically fitted function not the standard error of the mean.

³ not keeping into account that valpromide is metabolized to the corresponding valproic acid (Radatz et al., 1998) and therefore probably activated and intrinsically not active (also see results and discussion).

⁴ assumed that the solvent enhancer Chremophor EL 25 % (v/v) is reducing the teratogenic effect of the compound (also see results and discussion).

DMD #8078

Table 4 Plasma protein binding of S-2-pentyl-4-pentynoic hydroxamic acid and its metabolite S-2-pentyl-4-pentynoic acid in spiked human and mouse plasma.

	Plasma	Concentration of sample \pm SD ¹ (mg/mL)	Concentration of filtrate \pm SD ¹ (mg/mL)	Protein binding (%)
S-2-Pentyl-4-pentynoic acid IX	Control	670 \pm 19 65 \pm 3	681 \pm 8 66 \pm 3 Average	0 0 0
	Mouse	951 \pm 49 852 \pm 57 221 \pm 6 72 \pm 12	464 \pm 36 236 \pm 37 61 \pm 7 15 \pm 2 Average	51 72 72 80 69
	Human	821 \pm 19 684 \pm 24 261 \pm 7 60 \pm 3 25 \pm 1	202 \pm 6 128 \pm 7 17 \pm 2 < LOD < LOD Average	76 82 95 100 100 91
S-2-Pentyl-4-pentynoic hydroxamic acid X	Control	281 \pm 8	278 \pm 17 Average	0 0
	Mouse	326 \pm 5 73 \pm 3	188 \pm 12 38 \pm 1 Average	42 48 45
	Human	889 \pm 17 366 \pm 6 84 \pm 3	309 \pm 5 84 \pm 3 11 \pm 1 Average	65 77 87 76

¹ with n=4 samples each

Table 5 Concentrations in plasma and tissue of NMRI mice treated with either 0.80 mmol/kg S-2-pentyl-4-pentynoic hydroxamic acid (i.p.) or 1.50 mmol/kg S-2-pentyl-4-pentynoic acid (s.c.).

	Concentrations \pm SD at time points (min) after dosage (mg/mL or mg/g)								
	0	7	15	30	60	120	240	360	720
S-2-pentyl-4-pentynoic hydroxamic acid									
Plasma	< LOD	124 \pm 12	157 \pm 44	58 \pm 26	41 \pm 10	< LOD	< LOD	< LOD	< LOD
Brain	< LOD	141 \pm 12	186 \pm 42	74 \pm 8	38 \pm 14	< LOD	< LOD	< LOD	< LOD
Liver	< LOD	72 \pm 6	67 \pm 35	23 \pm 16	< LOQ	< LOD	< LOD	< LOD	< LOD
Kidney	n.d.	n.d.	n.d.	n.d.	n.d.	n.d.	n.d.	n.d.	n.d.
Spleen	< LOD	106 \pm 11	120 \pm 67	< LOQ	25 ¹	< LOD	< LOD	< LOD	< LOD
The metabolite S-2-pentyl-4-pentynoic acid									
Plasma	< LOD	41 \pm 2	65 \pm 6	112 \pm 10	106 \pm 21	114 \pm 5	29 \pm 8	32 \pm 14	< LOD
Brain	< LOD	14 \pm 3	18 \pm 8	29 \pm 11	24 \pm 7	20 \pm 2	< LOQ	< LOQ	< LOD
Liver	< LOD	156 \pm 2	122 \pm 28	123 \pm 18	95 \pm 3	58 \pm 5	28 \pm 8	34 \pm 15	< LOQ
Kidney	< LOD	65 \pm 7	61 \pm 13	78 \pm 14	75 \pm 14	74 \pm 8	14 \pm 4	44 \pm 31	< LOD
Spleen	< LOD	16 \pm 8	24 \pm 13	42 \pm 18	42 \pm 28	65 \pm 14	< LOQ	< LOQ	< LOD
S-2-pentyl-4-pentynoic acid									
Plasma	< LOD	501 \pm 85	530 \pm 64	570 \pm 55	555 \pm 30	439 \pm 8	226 \pm 70	267 \pm 18	< LOQ
Brain	< LOD	217 \pm 101	191 \pm 38	233 \pm 8	242 \pm 14	171 \pm 12	52 \pm 29	47 \pm 14	< LOQ
Liver	< LOD	375 \pm 57	368 \pm 79	421 \pm 80	617 \pm 66	411 \pm 56	201 \pm 50	143 \pm 32	38 \pm 21
Kidney	< LOD	223 \pm 34	300 \pm 88	275 \pm 11	514 \pm 110	352 \pm 84	162 \pm 80	165 \pm 48	17 ¹
Spleen	< LOD	150 \pm 16	154 \pm 43	225 \pm 48	416 \pm 75	221 \pm 41	83 \pm 52	68 \pm 17	< LOQ

¹ n=1

DMD #8078

Table 6 Pharmacokinetic parameters of S-2-pentyl-4-pentynoic hydroxamic acid, its metabolite S-2-pentyl-4-pentynoic acid, and valproic acid (Radatz et al. 1998) in the NMRI mouse model.

	S-2-Pentyl-4-pentynoic hydroxamic acid X	S-2-Pentyl-4-pentynoic acid IX	Valproic acid I
Dosage (mmol/kg)	0.80	1.50	3.00
C_{max} (µg/mL)	230	630	730
t_{max} (µg/mL)	15	30	15
t_{1/2} (h)	0.33	4.24	1.40
AUC_{0-∞} (h*µg/mL)	100	3443	1748
V_z (L/kg)	0.733	0.454	--
Cl (mL/h/kg)	1466	67	--
MRT (h)	0.54	6.22	--

Table 7 Reproductive toxicity assessment of *R*- and *S*-2-pentyl-4-pentynoic hydroxamic acid as measured in the NMRI-*exencephaly*-mouse-model.

Compound	Dose (mmol/kg)	Fetal weight \pm SD (g)	Litters (N)	Living embryos (N)	Embryo lethality (%)	Exencephaly rate (%)
<i>S</i> -2-pentyl-4-pentynoic hydroxamic acid X	1.50 ^a	1.12 \pm 0.19 ^c	6	66	21 ^e	5
	1.00 ^a	1.16 \pm 0.15 ^c	5	69	9 ^e	0
	0.80 ^b	1.19 \pm 0.18 ^c	5	54	19^f	2
<i>R</i> -2-pentyl-4-pentynoic hydroxamic acid VIII	1.50 ^a	1.20 \pm 0.13 ^c	5	53	11 ^e	0
	1.00 ^a	1.18 \pm 0.12 ^c	3	44	3 ^e	0
	0.80 ^b	1.23 \pm 0.12^d	6	80	3 ^e	0
Control A (CremEL 25% pH 7.4)	a	1.17 \pm 0.14	13	159	13	0
Control B (NaCl, 8.0 g/L, pH 7.4)	b	1.15 \pm 0.13	6	77	5	0

^a Compound was dissolved in CremEL 25% v/v and neutralized

^b Compound was dissolved in Water and neutralized

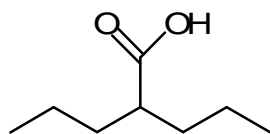
^c Data were not distributed normally (Kolmogorov-Smirnov test) and not significantly different to control (Anova on ranks, Dunns Method)

^d Data were not distributed normally (Kolmogorov-Smirnov test) but significantly different to control $p < 0.05$ (Anova on ranks, Dunns Method)

^e Data were not significantly different to control (t-test)

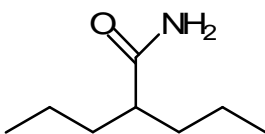
^f Data were significantly different to control with $p < 0.05$ (z-test)

Figure 1



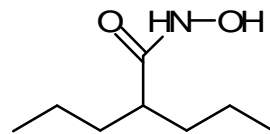
Valproic acid, VPA

I



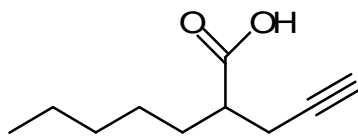
Valpromide, VPD

II



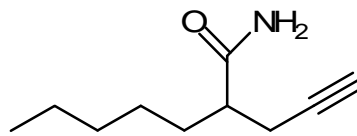
Valproic hydroxamic acid, VPA-HA

III



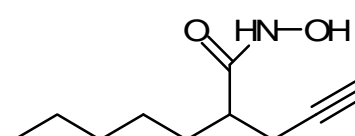
(±)-2-pentyl-4-pentynoic acid

IV



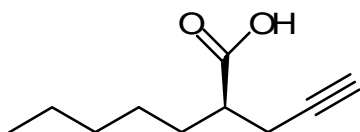
(±)-2-pentyl-4-pentynoic amide

V



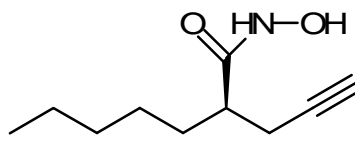
(±)-2-pentyl-4-pentynoic hydroxamic acid

VI



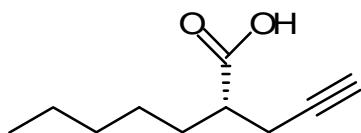
(R)-2-pentyl-4-pentynoic acid

VII



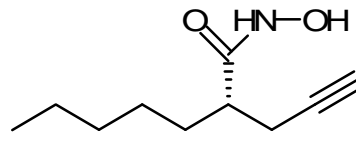
(R)-2-pentyl-4-pentynoic hydroxamic acid

VIII



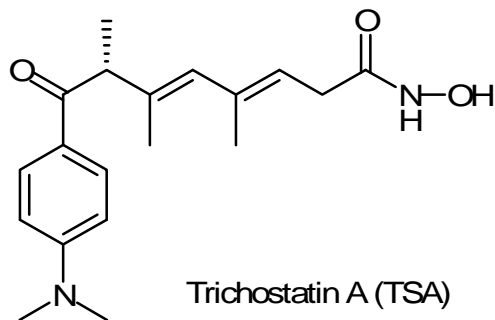
(S)-2-pentyl-4-pentynoic acid

IX

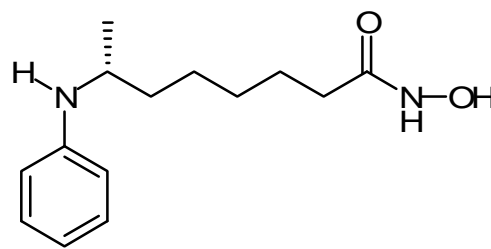


(S)-2-pentyl-4-pentynoic hydroxamic acid

X



Trichostatin A (TSA)



Suberoylanilidehydroxamic acid (SAHA)

Figure 2

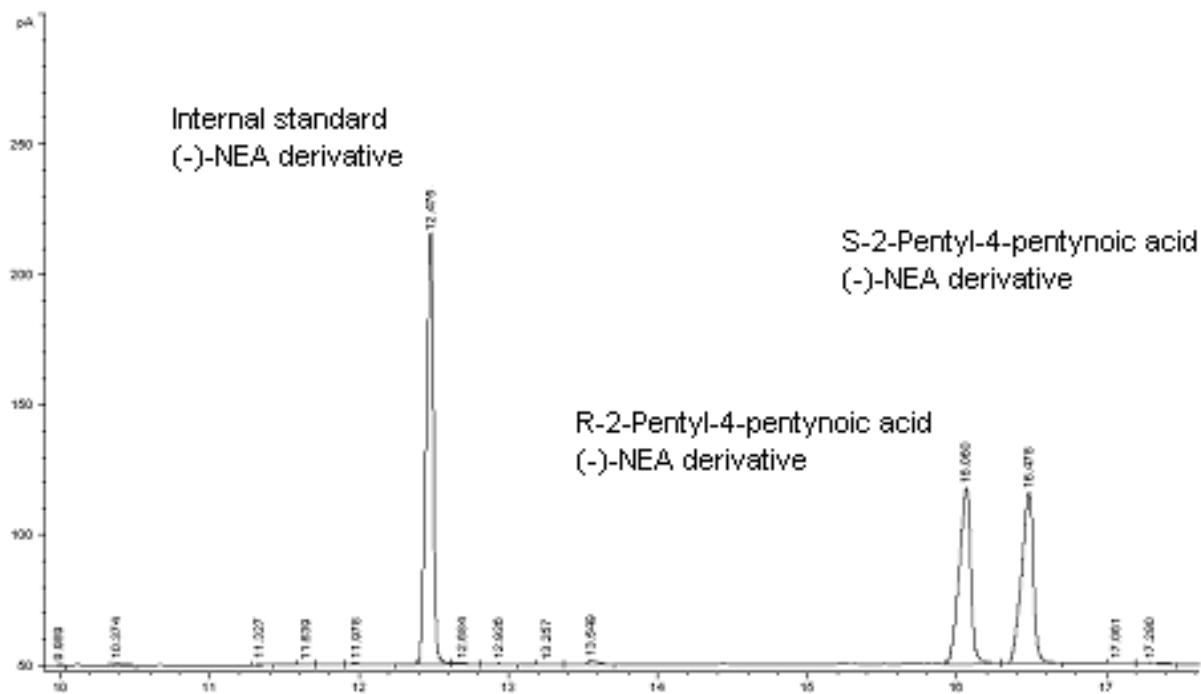
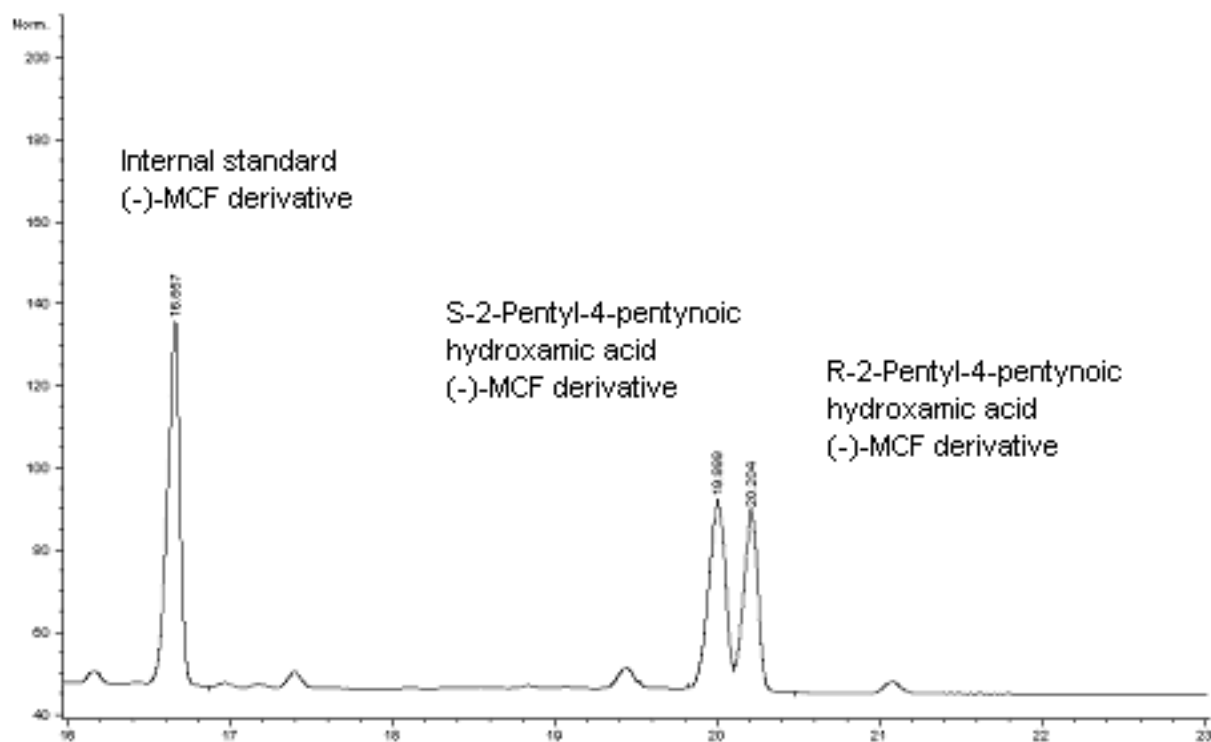


Figure 3

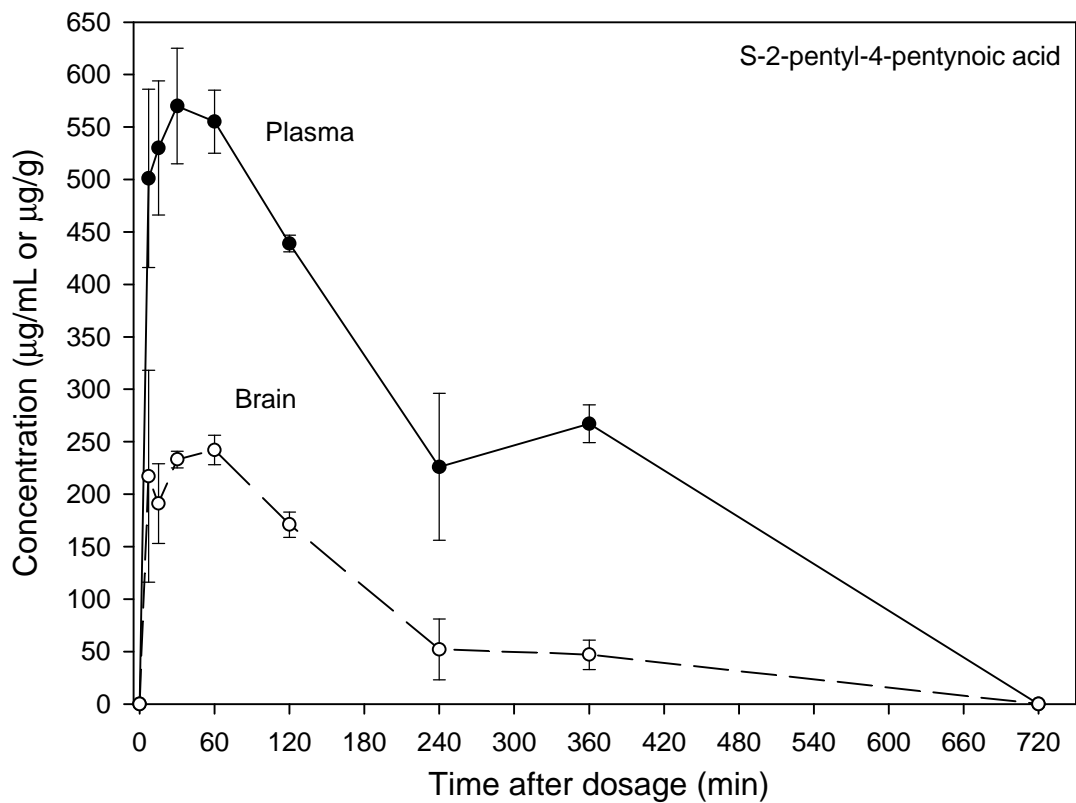
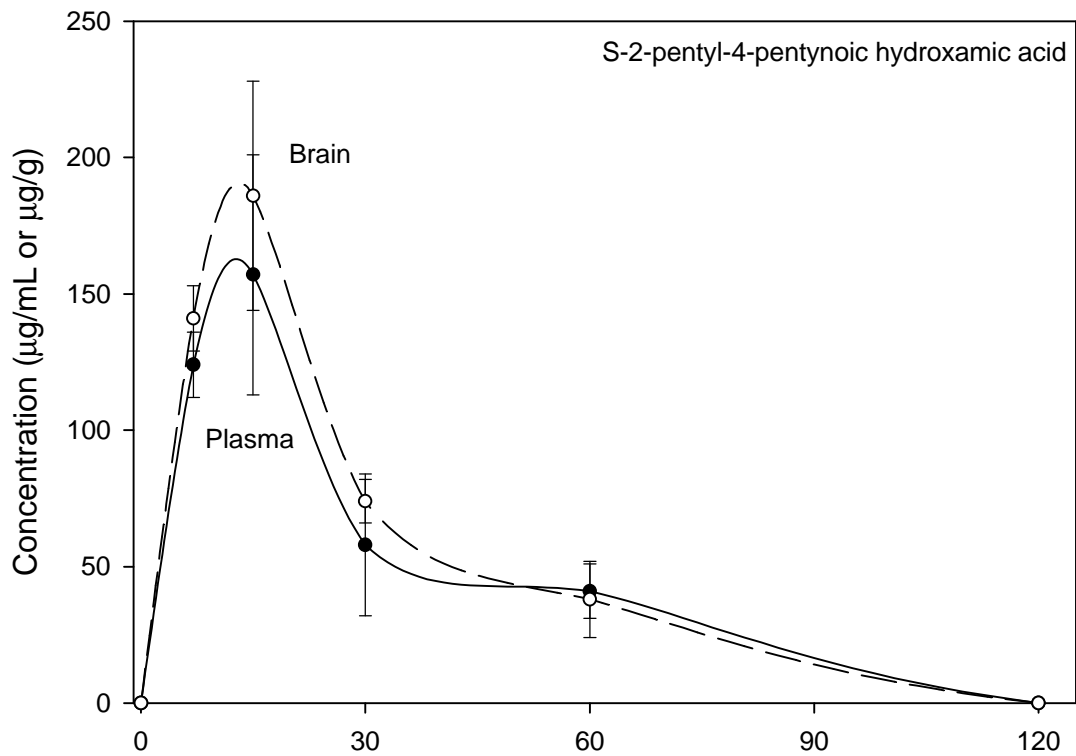


Figure 4

